

## Spin-Lattice Relaxation Time of Ferromagnetic Gadolinium Determined with Time-Resolved Spin-Polarized Photoemission

A. Vaterlaus, T. Beutler, and F. Meier

*Laboratorium für Festkörperphysik, Eidgenössische Technische Hochschule Hönggerberg, CH-8093 Zürich, Switzerland*  
(Received 29 May 1991)

The characteristic time for establishing thermal equilibrium between the lattice and the spin system is  $100 \pm 80$  ps in ferromagnetic gadolinium.

PACS numbers: 78.47.+p, 75.50.Cc, 79.20.Ds, 79.60.Cn

Upon a sudden change of the lattice temperature, a magnet needs time to establish its new equilibrium magnetization. The characteristic time—known as spin-lattice relaxation time  $\tau_{SL}$ —measures the strength of the coupling between the spin system and the lattice. Apart from its evident physical interest, this quantity is technologically important because it determines, for instance, the maximum speed attainable in Curie-point writing, the most widely applied technique of magneto-optical recording.

Because of the lack of appropriate experimental tools, the spin-lattice relaxation time in ferromagnets has not been determined so far. Only upper and lower limits have been given for Ni [1] and for Fe [2]. In the present paper, it is demonstrated that  $\tau_{SL}$  can be measured using the technique of time-resolved spin-polarized photoemission.

The lattice is heated with a laser pulse of 10 ns duration. The photon energy is less than the photothreshold of the sample. Accordingly, this pulse does not emit photoelectrons [3]. The temporal evolution of the magnetization during the ns-heating pulse is probed by measuring the spin polarization of the electrons emitted by a second, synchronized laser pulse of 60 ps duration and a photon energy above photothreshold. Since the time interval between the onset of the heating and the probing pulse is adjustable with ps accuracy, the variation of the magnetization can be measured as a function of time. Thus, the photoemission experiment becomes time resolved, i.e., capable of monitoring the dynamics of fast, transient phenomena. The relaxation time for Gd is found to be  $100 \pm 80$  ps. There are no basic experimental restrictions for applying the technique to other ferromagnetic or ferromagnetic materials.

For continuous light sources, the spin-polarized photoemission experiment is described in Ref. [4]; for pulsed lasers, in Ref. [5]. It is proved that, and understood why, laser-induced spin-polarized photoemission is insensitive to space charge, a basic requirement for performing the experiment successfully. All the emitted electrons are collected and directed into a 100-kV Mott detector in order to measure the spin polarization  $P = (N_{\uparrow} - N_{\downarrow}) / (N_{\uparrow} + N_{\downarrow})$  where  $N_{\uparrow}$  ( $N_{\downarrow}$ ) is the number of electrons with spin magnetic moment parallel (antiparallel) to the surface normal of the sample. Along this direction an

external magnetic field  $\leq 3$  T can be applied. The temperature of the sample is variable between 30 K and several hundred K.

Gd was deposited onto a polycrystalline iron substrate (conically shaped, 6 mm long, exposed surface; 4 mm diameter) by evaporation from a resistively heated W spiral. Extensive outgassing was necessary in order to produce clean Gd films. Before deposition, the iron substrate was cleaned by sputtering and heating cycles. Film and substrate quality were tested with Auger spectroscopy. After deposition of Gd, the Fe Auger signal was completely suppressed, giving a lower limit of 50 Å for the Gd film thickness. Figure 1 shows the spin polarization of the photoelectrons as a function of the perpendicularly applied magnetic field at  $T = 45$  K. Saturation occurs for fields exceeding 0.38 T. This small saturation field is due to the enhancement of the external field by the iron substrate.

Because of the surface sensitivity of the photoemission experiment [6], the measured polarization reflects the magnetic state of the Gd film only. The temperature dependence of the polarization is shown in Fig. 2. A linear extrapolation of the curve gives a Curie temperature of 290 K. This value is in agreement with previous photoemission experiments [7] and with the bulk Curie temperature of Gd [8]. For the experiments displayed in

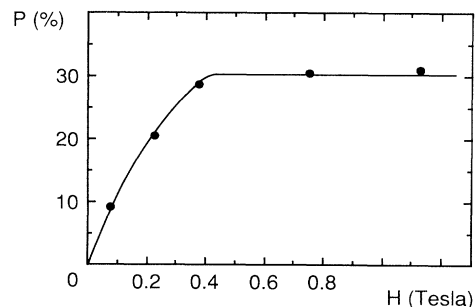


FIG. 1. Spin polarization  $P$  of the photoelectrons emitted from a Gd film as a function of the external field  $H$  applied perpendicularly to the sample surface. The full spectrum of a Hg-Xe lamp ( $h\nu \leq 5.5$  eV) is used as a light source. Complete alignment of the magnetization along the surface normal is achieved for external fields exceeding 0.38 T. The temperature is 45 K. The sample has a photothreshold of 3 eV.

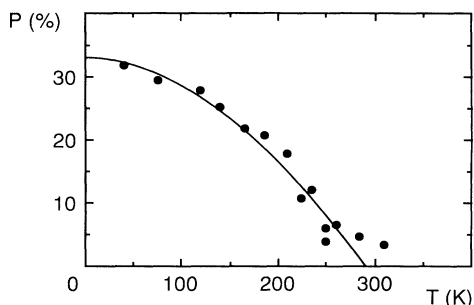


FIG. 2. Saturation polarization  $P$  of the photoelectrons measured as a function of the temperature. Saturation is achieved by applying an external field of 0.38 T. The full spectrum of a Hg-Xe lamp ( $h\nu \leq 5.5$  eV) is used as a light source. The Curie temperature is 290 K.

Figs. 1 and 2, the full spectrum of a Hg-Xe lamp ( $h\nu \leq 5.5$  eV) has been used. The photothreshold of the Gd film was 3 eV.

For generating the time-delayed laser pulses, the output of a pulsed KrF-excimer laser ( $h\nu = 5$  eV) is fed into a beam splitter. One of the emerging beams is guided over a variable optical delay before it pumps a 10-ns dye laser of 2.15-eV photon energy. This heating pulse is focused onto the sample surface where it raises the lattice temperature—depending on the pulse energy—up to several hundred degrees. The other excimer beam pumps a 60-ps dye laser having a photon energy of 3.2 eV. This pulse hits the sample surface in the center of the heating pulse where it probes the magnetization via emission of polarized photoelectrons. By varying the optical delay, i.e., the path length of the pump beam for the ns laser, the onset of the probing pulse can be moved from 2.5 ns before to 7 ns after the onset of the heating pulse.

Time-resolved measurements at two different intensities of the heating pulse are shown in Figs. 3(a) and 3(b). The normalized polarization  $P/P_0$  ( $P_0 = 38\%$ ) measured at  $t \leq 0$  corresponds to the equilibrium magnetization at the initial temperature  $T_0 = 45$  K. The previously found saturation field of 0.38 T is applied perpendicular to the sample surface. The external field and the probing spot (diameter 360  $\mu\text{m}$  FWHM) both limit the area from which the photoelectrons are collected to 270  $\mu\text{m}$  (FWHM). Since the focus of the heating pulse has a diameter of 390  $\mu\text{m}$ , the area which contributes to the photoelectric current is nearly homogeneously heated. Note that no measurable change of the spin polarization—or, equivalently, of the magnetization—occurs due to heating by the probing pulse itself. Using 30-ps pulses, it has been shown in Ref. [2] that electrons emitted by a single pulse (no heating by a previous, first pulse) retain the polarization of the prepulse, undisturbed state even if the pulse energy is sufficient to melt the surface, a result which is corroborated by the time-resolved measurements reported in this paper. Neither the heating nor the probing pulse caused damage to the surface, as recognized by

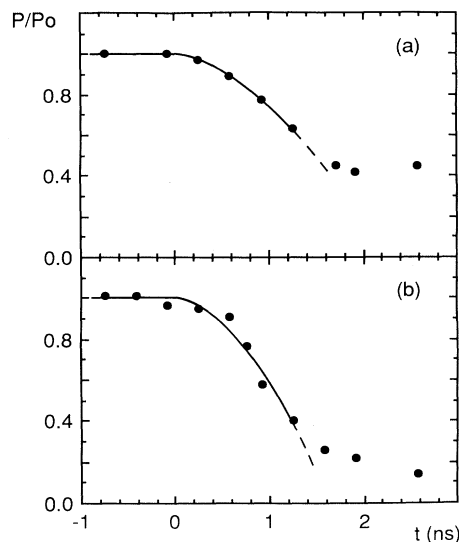


FIG. 3. Pump-probe experiment using a 60-ps (3.2 eV) laser pulse as the probing pulse and a 10-ns (2.15 eV) laser pulse as the heating pulse. The reduced spin polarization of the photoelectrons emitted by the probing pulse is plotted as a function of the time delay between probing and heating pulses. Zero time delay corresponds to the onset of the lattice heating. Solid lines: calculated  $P(t)$  curves involving no adjustable parameters (see text).

the complete reversibility of the  $P(t)$  measurements. Particularly for Gd this is understandable because the pulse energy required to reach the Curie temperature is a factor of 5 lower than that necessary for melting.

Qualitatively, the effect of laser heating is apparent in both  $P(t)$  curves shown in Fig. 3: For  $t > 0$  the polarization drops. The measurements differ in the energy of the heating pulse. In Fig. 3(a), the energy of the heating pulse is modest: It is just sufficient to reduce the initial-state polarization by a factor of 0.4. In Fig. 3(b), the heating pulse energy is higher, raising the spin temperature close to the Curie temperature. Measurements taken at other heating pulse energies and initial temperatures of the sample will be reported in a forthcoming paper [9].

In Fig. 3(a), the polarization drops from  $P/P_0 = 1.0$  to a constant value of 0.4. This corresponds—according to Fig. 2—to a temperature rise of  $175 \pm 10$  K. The fact that—on the time scale of Fig. 3— $P/P_0$  reaches a constant value is a consequence of the particular temporal intensity profile of the heating pulse shown in Fig. 4 by the solid circles [10]. The intensity scale on the left of the figure applies to the pulse energy of Fig. 3(a).

The temperature rise  $\Delta T_{\text{lattice}}$  can be derived from the temporal intensity profile of the laser pulse using the classical thermal-diffusion equation [11]. The reason is that in our experiment the duration of the heating pulse is much longer than the characteristic time needed to transfer the pulse energy to the lattice, a time which is of

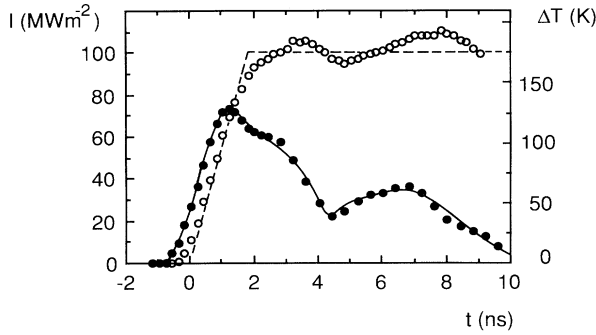


FIG. 4. Solid circles: Intensity of the heating laser pulse [of the measurement in Fig. 3(a)] as a function of time (left-hand scale). Using the solid line as a fit through the solid circles, the temperature rise  $\Delta T_{\text{lattice}}$  induced by the heating laser is calculated.  $\Delta T_{\text{lattice}}$  is displayed by the open circles (right-hand scale).

the order of 1 ps [12–14].

The result of solving the thermal-diffusion equation is shown in Fig. 4 by the open circles. The linear increase of the intensity at the front end of the laser pulse transforms into a linear rise of  $T_{\text{lattice}}$  over this time interval. Accidentally, the pulse profile causes  $T_{\text{lattice}}$  to level off after the linear rise and this is, of course, the reason that  $P/P_0$  also reaches the constant value of 0.4 in Fig. 3(a). A glance at  $P(t)$  in Fig. 3(a) and  $\Delta T_{\text{lattice}}(t)$  in Fig. 4 shows that the times where the two quantities reach constant values are very similar, slightly less than 2 ns. This implies that the spin and lattice temperatures are very close to each other on this time scale or, equivalently, it shows that the spin-lattice relaxation time  $\tau_{\text{SL}}$  must be far less than 2 ns.

Now, the temperature rise  $\Delta T_{\text{lattice}}(t)$  in Fig. 4 can be calibrated in degrees K, since one knows from the  $P(t)$  measurement of Fig. 3(a) that the total drop of the polarization ( $P/P_0 = 1.0 \rightarrow 0.4$ ) corresponds (according to Fig. 2) to a temperature rise of 175 K. In the plateau region, this temperature rise is identical for the spin and lattice temperatures. In passing, we note that solving the thermal-diffusion equation with the material parameters of the substrate, i.e., of Fe—taken at 140 K and assumed to be  $T$  independent [15]—yields a  $\Delta T_{\text{lattice}}(t)$  very close to the one determined experimentally from Fig. 3(a) [9].

Next, we derive a numerical value for  $\tau_{\text{SL}}$ . The rate equation for the temperature transfer between the spin system and the lattice is [16]

$$C_{\text{spin}} \frac{dT_{\text{spin}}}{dt} = G(T_{\text{lattice}} - T_{\text{spin}}). \quad (1)$$

$C_{\text{spin}}$  is the specific heat of the spin system and  $G$  is the phonon-magnon coupling constant. The characteristic time for the equilibration of the temperature is then given by

$$\tau_{\text{SL}} = C_{\text{spin}}/G. \quad (2)$$

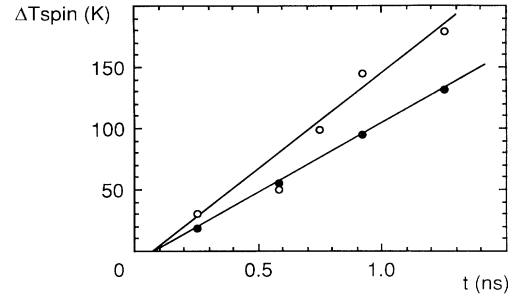


FIG. 5.  $\Delta T_{\text{spin}}(t)$  derived from Fig. 2 for the data of Fig. 3(a) (solid circles) and Fig. 3(b) (open circles). The straight lines correspond to the fit  $\Delta T_{\text{spin}}(t) = q(t - \tau_{\text{SL}})$ . The open-circle data point at 0.60 ns deviates from the straight line as does the corresponding measured polarization value in Fig. 3(b) from the  $P(t)$  curve.

$C_{\text{spin}}$  (not  $G$ ) depends on temperature. However, in the following,  $\tau_{\text{SL}}$  is understood to be a  $T$ -independent, averaged (for  $45 < T < 225$  K) quantity which makes it possible to solve Eq. (1) analytically. Guided by Fig. 4, the lattice temperature is taken to increase linearly in time,  $T_{\text{lattice}} = T_0 + qt$ , where  $T_0$  is the initial temperature at  $t \leq 0$  and  $q$  is the rate of the temperature increase. Then, the solution of Eq. (1) is

$$T_{\text{spin}}(t) = T_0 + q[t - \tau_{\text{SL}}(1 - e^{-t/\tau_{\text{SL}}})]. \quad (3)$$

The quantity  $\Delta T_{\text{spin}}(t) = T_{\text{spin}}(t) - T_0$  is derived exclusively from experimental data: Figure 3 gives the polarization at a time  $t$  after the lattice heating has started. The corresponding increase  $\Delta T_{\text{spin}}(t)$  of the spin temperature is obtained from Fig. 2. Notice the unique feature of the spin-polarized pump-probe experiment, namely, that the magnetization acts as a thermometer, indicating at each instant of time the spin temperature. Unfortunately, for the lattice and electron gas similarly simple thermometers do not exist.

$\Delta T_{\text{spin}}(t)$  is plotted in Fig. 5 for both measurements of Fig. 3. Equation (3) shows that  $\Delta T_{\text{spin}}(t) = q(t - \tau_{\text{SL}})$  for  $t > \tau_{\text{SL}}$ . Indeed, this linear relationship is found in Fig. 5. Extrapolation of the straight lines to  $\Delta T_{\text{spin}} = 0$  gives—independent of  $q$ —an intersection with the time axis at  $t = \tau_{\text{SL}}$ . In this way  $\tau_{\text{SL}}$  is found and it amounts to  $100 \pm 80$  ps for both measurements shown in Fig. 3 [17].

The zero of the time scale in Fig. 5 is obtained from a  $P(t)$  measurement at high heating pulse energy [9]. It must lie between the last point where  $P/P_0 = 1$  and the first point where  $P/P_0 < 1$ . The error in  $\tau_{\text{SL}}$  of  $\pm 80$  ps is mainly due to the uncertainty of the zero point of the time scale.

The rate of the temperature increase is given by the slope of the straight lines in Fig. 5; it is  $q = 115$  K/ns and  $q = 158$  K/ns for the measurements of Figs. 3(a) and

3(b), respectively.

Using these experimentally determined values of  $\tau_{SL}$  and  $q$  together with the  $P(T)$  relation from Fig. 2, the curves  $P(t)$  are obtained immediately using Eq. (3). The result is shown as the solid lines in Fig. 3. Evidently, the fit—without any adjustable parameter—is perfect.

This paper reports on the first experiments where the time evolution of the magnetic nonequilibrium state has been followed on a picosecond time scale. The novel technique used is time-resolved spin-polarized photoemission, using pulsed lasers as light sources. The characteristic time for the heat transfer from the lattice to the spin system has been found to be  $100 \pm 80$  ps in ferromagnetic gadolinium.

We thank H. C. Siegmann for his continuous interest and encouragement. The expert technical assistance by K. Brunner was crucial for the successful completion of this experiment. The financial support by the Schweizerische Nationalfonds is gratefully acknowledged.

- 
- [1] M. B. Agranat, S. I. Ashitkov, A. B. Granovskii, and G. I. Rukman, *Zh. Eksp. Teor. Fiz.* **86**, 1376 (1984) [*Sov. Phys. JETP* **59**, 804 (1984)].
  - [2] A. Vaterlaus, D. Guarisco, M. Lutz, M. Aeschlimann, M. Stampanoni, and F. Meier, *J. Appl. Phys.* **67**, 5661 (1990).
  - [3] The absence of heating-pulse-induced multiphoton-multilevel photoelectron excitation requires a separate check; if emission occurs, it must be suppressed by varying the photon energy.
  - [4] M. Campagna, D. T. Pierce, F. Meier, K. Sattler, and H. C. Siegmann, *Adv. Electron. Electron Phys.* **41**, 113 (1976).
  - [5] G. L. Bona, F. Meier, G. Schönhense, M. Aeschlimann, M. Stampanoni, G. Zampieri, and H. C. Siegmann, *Phys. Rev. B* **34**, 7784 (1986); F. Meier, A. Vaterlaus, M.

- Aeschlimann, M. Lutz, D. Guarisco, F. Milani, and H. C. Siegmann, *J. Magn. Magn. Mater.* **91**, 314 (1991).
- [6] D. Pescia, M. Stampanoni, G. L. Bona, A. Vaterlaus, R. F. Willis, and F. Meier, *Phys. Rev. Lett.* **58**, 2126 (1987).
- [7] A. Cerri, D. Mauri, and M. Landolt, *Phys. Rev. B* **27**, 6526 (1983).
- [8] James J. Rhyne, in *Magnetic Properties of Rare Earth Metals*, edited by R. J. Elliot (Plenum, New York, 1972), p. 132.
- [9] A. Vaterlaus, T. Beutler, and F. Meier (to be published).
- [10] The temporal intensity profile of the heating pulse has been measured using an ITL TF 1850 vacuum photodiode (rise time 100 ps) and a Tektronix 2467 350-MHz oscilloscope.
- [11] J. H. Bechtel, *J. Appl. Phys.* **46**, 1585 (1975).
- [12] J. G. Fujimoto, J. M. Liu, E. P. Ippen, and N. Bloembergen, *Phys. Rev. Lett.* **53**, 1837 (1984).
- [13] H. E. Elsayed-Ali, T. B. Norris, M. A. Pessot, and G. A. Mourou, *Phys. Rev. Lett.* **58**, 1212 (1987).
- [14] R. W. Schoenlein, W. Z. Lin, J. G. Fujimoto, and G. L. Eesley, *Phys. Rev. Lett.* **58**, 1680 (1987).
- [15] The material parameters of iron are thermal conductivity, 1.14 W/cmK; thermal diffusivity, 0.26 cm<sup>2</sup>/s; optical-absorption coefficient for the wavelength of the heating laser,  $6.59 \times 10^5$  cm<sup>-1</sup>; and surface reflectivity, 0.52. The laser parameters are  $h\nu = 2.15$  eV; pulse energy, 67.6  $\mu$ J [heating pulse energy of measurement Fig. 3(a)]; focus diameter (FWHM), 390  $\mu$ m; and temporal intensity profile (see solid line in Fig. 4). If the material parameters of Gd were taken, the calculated temperature rise would be larger but would keep its temporal profile.
- [16] S. I. Anisimov, B. L. Kapeliovich, and T. L. Perel'man, *Zh. Eksp. Teor. Fiz.* **66**, 776 (1974) [*Sov. Phys. JETP* **39**, 375 (1974)].
- [17] From Fig. 5, the duration of the linear increase of the lattice temperature is found to be 1.5 ns, whereas from Fig. 4 this time interval appears instead to be 1.8 ns. The reason for the different times is instrumental broadening of the measurements in Fig. 4 (see Ref. [10]).